Malaysian Journal of Chemistry, 2021, Vol. 23(4), 49-55
(Special Issue: 3rd Virtual Symposium on Multidisciplinary Science 2021 (V-SMS2021))

Borazine as Alternative to Benzene-based Organic Linkers for Gas Adsorption on Metal-Organic Frameworks

Mostafa Yousefzadeh Borzehandani[1,2], Emilia Abdulmalek[1,2], Mohd Basyaruddin Abdul Rahman[1,2] and Muhammad Alif Mohammad Latif[1,3]*
[1]Integrated Chemical BioPhysics Research, Faculty of Science, Universiti Putra Malaysia,
43400 UPM Serdang, Selangor, Malaysia
[2]Department of Chemistry, Faculty of Science, Universiti Putra Malaysia,
43400 UPM Serdang, Selangor, Malaysia
[3]Centre of Foundation Studies for Agricultural Science, Universiti Putra Malaysia,
43400 UPM Serdang, Selangor, Malaysia
*Correspondence author (e-mail: aliflatif@upm.edu.my)

Metal-organic frameworks (MOFs) are porous materials that are extensively used for gas adsorption and storage due to their unique features. The use of borazine in the construction of MOFs (instead of the more common organic fragment, benzene) offers an ideal solution to overcome challenges that arise from functionalizing MOFs. In this study, we modified the original HKUST-1 MOF by replacing the benzene ring in the organic linker with borazine. The adsorption of greenhouse gases by both HKUST-1 and borazine-based HKUST-1 (hB-HKUST-1) were studied. The adsorption of CO_2 and CH_4 by both MOFs were simulated at 298 K over a range of pressures (0-160 kPa) using grand canonical Monte Carlo simulations. hB-HKUST-1's surface enhanced the adsorption of CO_2 gas, but did not influence the adsorption of CH_4. The isosteric heats of adsorption (Q_{st}) demonstrated higher CO_2 adsorption by both frameworks compared to CH_4. CO_2 gas also showed higher loadings of 188.4 and 204.9 mg.g^{-1}, respectively, in HKUST-1 and hB-HKUST-1. Analysis of interaction energies revealed that adsorbent–adsorbate interactions were as much determinative as adsorbate–adsorbate interactions. Snapshots from the simulation indicated that CO_2 molecules preferred smaller pores. This valuable information can be a guideline to produce borazine-based MOFs for better gas absorption and storage.

Key words: HKUST-1; borazine; metal-organic framework; gas absorption; grand canonical Monte Carlo

Received: June 2021; Accepted: October 2021

In the last two decades, metal-organic frameworks (MOFs) have emerged as functional porous materials for adsorption and storage of greenhouse gases [1], [2]. The outstanding characteristics of MOFs in gas-related applications are reflected by their high surface area, high thermal and chemical stability, recyclability and a high degree of structural tunability [3]. The structural tunability of MOFs for greenhouse gas adsorption is commonly developed using a functionalization approach [4]. Incorporating large van der Waals and highly polar functional groups on MOFs' organic linkers increased interactions and the adsorption of gas molecules. For instance, the methyl-functionalized UiO-66 exhibited van der Waals interactions and selectivity for a CO_2/CH_4 mixture as good as UiO-66 under dry conditions [5]. Also, the amine-functionalized IRMOF-3 showed a remarkable selectivity for CO_2 compared to its parent framework [6]. In spite of the great efficiency of functionalization strategies for gas adsorption, there are still some serious challenges: i) functionalized organic linkers may be chemically affected by solvents during synthesis which may lead to unwanted crystal structures [7], and ii) post-synthesis modification (PSM) for MOFs with high concentrations of coordinatively unsaturated metal sites (CUMs) imposes limitations, because functional groups would preferably interact and accumulate on CUMs [8].

Borazine was first introduced by Alfred Stock and Erich Pohland in 1926 [9]. Borazine is built with an equivalent bond length (1.429) as a hexagonal ring that is polar, rigid and planar. It is also commonly known as inorganic benzene [10], [11]. Employing borazine as an organic linker fragment may reduce problems associated with functionalization. Consequently, we have attempted to modify a MOF using borazine rings to examine its gas adsorption behaviour in comparison with the parent MOF. HKUST-1 (Hong Kong University of Science and Technology) [12] was a suitable choice as it was rationally designed with tritopic organic linkers and this allowed borazine rings to connect to three sides with boron atoms [13] (Figure 1). HKUST-1 features

---

†Paper presented at the 3rd Virtual Symposium on Multidisciplinary Science 2021 (V-SMS2021)

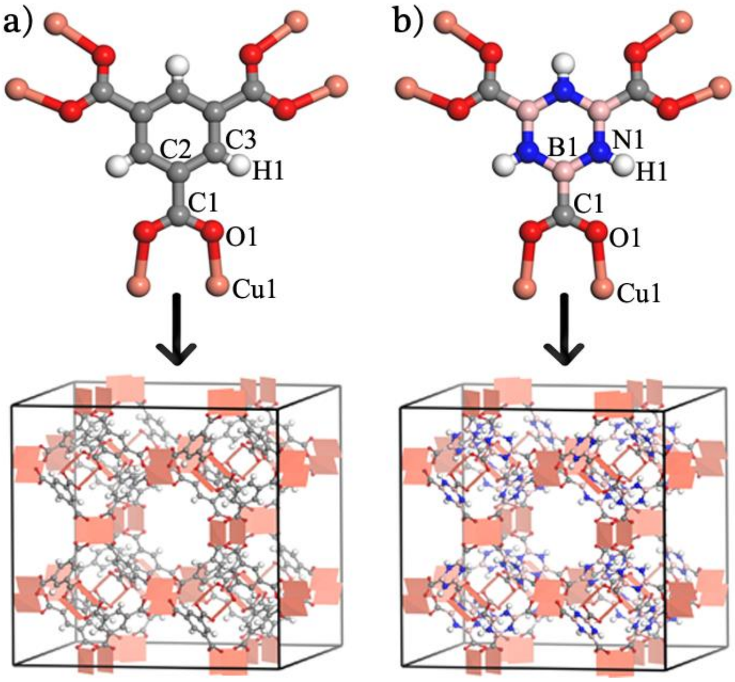

Figure 1. Asymmetric units of HKUST-1 (a) and hB-HKUST-1 (b), with their atom types labelled. The corresponding MOFs are shown in the respective boxes.

two types of pores, a larger pore aperture (14 Å) and a smaller pore aperture (10 Å) [14]. Here we propose a hypothetical MOF, in which the benzene ring in the HKUST-1 organic linker is replaced with borazine (hB-HKUST-1). To compare the capability of HKUST-1 and hB-HKUST-1 for greenhouse gas (CO_2 and CH_4) adsorption, we employed the grand canonical Monte Carlo (GCMC) simulation method. Identifying the interactions of gas molecules inside MOFs with experimental equipment is quite difficult. Such studies are better implemented on an atomic level by means of molecular simulations, which have an important role in the rational design and improvement of new MOFs.

Computational details

GCMC simulations were carried out using the RASPA 2.0 program [15] with the aim of investigating the adsorption of CO_2 and CH_4 into HKUST-1 and hB-HKUST-1. The crystal structure of HKUST-1 was obtained from the Cambridge Crystallographic Data Centre (CCDC code of 943009) [16]. In order to create hB-HKUST-1, the parent was modified by replacing the carbon atoms of the benzene ring with boron and nitrogen atoms. Adsorbent-adsorbate and adsorbate-adsorbate interactions were treated using Lennard-Jones (LJ) and Coulomb potentials. The parameters for the frameworks and gases were obtained from GenericMOFs [15] and TraPPE [17] force fields, respectively. Electrostatic interactions were determined using the Ewald summation method. Atomic charges for the gases and the periodic frameworks were computed using the charge equilibration (Qeq) method [18]. Periodic boundary conditions were applied in all directions in the simulation box. Up to 1×10^5 Monte Carlo cycles were considered for the simulation in which 5×10^4 cycles were initially set for equilibrium and 5×10^4 cycles were applied for the production phase. All simulations were performed at room temperature (298 K) and a range of pressures (0, 20, 40, 60, 80, 100, 120, 140 and 160 kPa) [19]. In this study, adsorption isotherms were evaluated at room temperature and low pressure, because we were interested in determining how the chemical composition of the frameworks affected gas adsorption [20]. The outcomes were used to explore radial distribution functions (RDF), theoretical maximum loading, isosteric heats of adsorption (Q_{st}), interaction energies and snapshot analyses.

RESULTS AND DISCUSSION

RDF is a valuable tool to detect the distribution of the gases in frameworks [21]. Figure 2 shows selected RDF plots for CO_2 and CH_4 in HKUST-1 and hB-HKUST-1. The carbon atoms in CO_2 had a higher distribution on the carbon atoms of phenyl ring in HKUST-1 compared to other atoms in HKUST-1 (Figure 2a). Also, carbon atoms in CO_2 showed a higher distribution on boron and hydrogen atoms compared to other sites in hB-HKUST-1 (Figure 2b). However, CO_2 reached its RDF peak in hB-HKUST-1 (at 3 and 4.5 Å). In the same manner of CO_2 gas in HKUST-1, the hydrogen atoms of CH_4 showed their highest peak on the phenyl ring in HKUST-1 (Figure 2c). The comparison of CH_4 in HKUST-1 and hB-HKUST-1 did not show any significant differences.

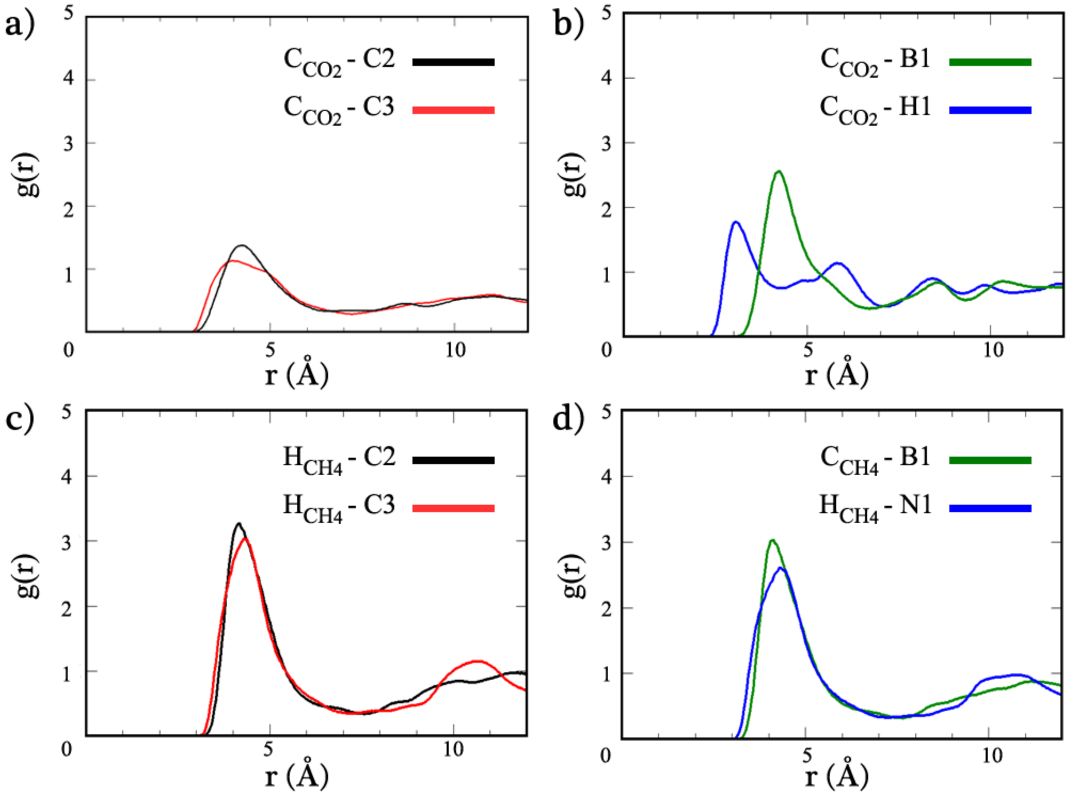

Figure 2. RDF plots for a) CO_2 in HKUST-1, b) CO_2 in hB-HKUST-1, c) CH_4 in HKUST-1 and d) CH_4 in hB-HKUST-1

The hydrogen atoms of CH_4 were well distributed on nitrogen and boron atoms in hB-HKUST-1, with almost the same peak intensity as in HKUST-1. The results of the RDF plots showed that there was no significant difference in the adsorption of CH_4 by HKUST-1 and hB-HKUST-1. In contrast, the two MOF structures had different CO_2 adsorption profiles, while hB-HKUST-1 produced stronger interactions with CO_2 gas molecules compared to HKUST-1.

To calculate the theoretical maximum loading, the two frameworks were exposed to an increasing amount of CO_2 and CH_4 under pressures of up to 160 kPa. Both gases gradually loaded into the MOF’s pores, although the values for CO_2 were about 10 times higher compared to those for CH_4 (Figure 3). A maximum loading of 188.4 mg.g^{-1} (41 mol/unit cell) and 204.9 mg.g^{-1} (45 mol/unit cell) was recorded for CO_2 in HKUST-1 and hB-HKUST-1, respectively, whereas the maximum loading of CH_4 was 21.2 mg.g^{-1} (12 mol/unit cell) and 19.8 mg.g^{-1} (12 mol/unit cell) in HKUST-1 and hB-HKUST-1, respectively. hB-HKUST-1 exhibited better loading with increasing CO_2 pressure. In contrast, HKUST-1 recorded a better loading for CH_4.

The isosteric heat of adsorption (Q_{st}) is attributed to the interaction between the adsorbed gas and the surface of the adsorbent. In this study, the Q_{st} values showed positive trends with pressure for CO_2 and CH_4 in HKUST-1 and hB-HKUST-1 (Figure 4). The Q_{st} values were positive for all pressures, indicating that the adsorption process was endothermic. After CO_2 loading, the MOFs experienced almost constant Q_{st} values of 20.7–22.9 and 22.2–24.3 kJ.mol^{-1} in HKUST-1 and hB-HKUST-1, respectively, over a range of pressures. On the other hand, CH_4 gases demonstrated a slight decline ranging from 18.5 to 15.0 and from 17.8 to 15.3 kJ.mol^{-1} in HKUST-1 and hB-HKUST-1, respectively. On comparing the frameworks, hB-HKUST-1 showed higher Q_{st} values, which can be attributed to a better surface provided by the borazine rings for interacting with CO_2, compared to HKUST-1. Like the RDF results, these two MOFs did not show considerable differences in their Q_{st} values for the adsorption of CH_4 over the range of pressures studied here.

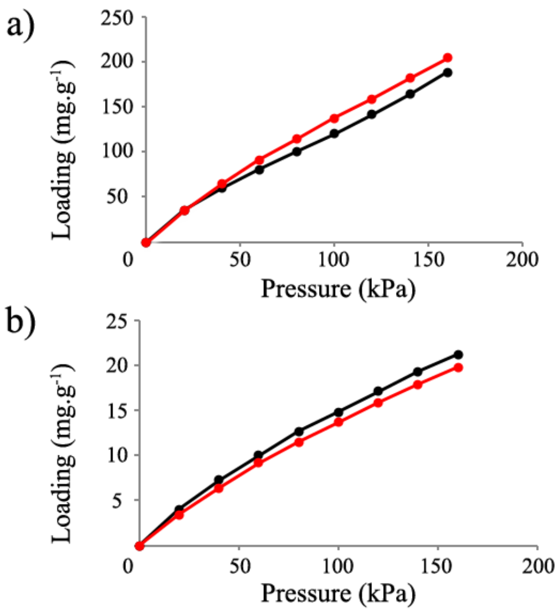

Figure 3. Maximum loading versus pressure for a) CO_2 and b) CH_4, in HKUST-1 (black lines) and hB-HKUST-1 (red lines)

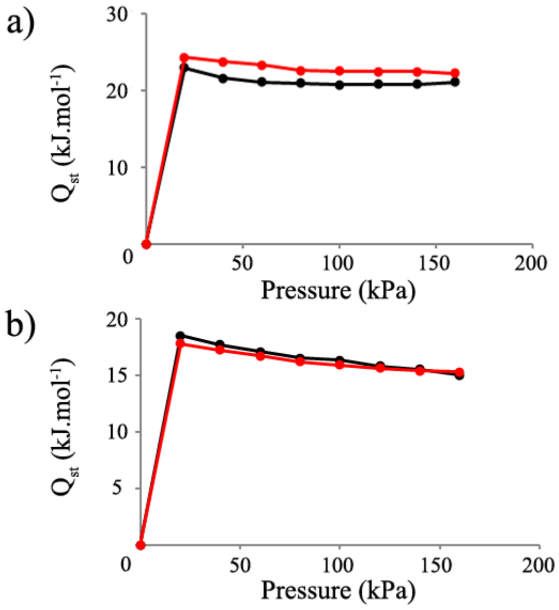

Figure 4. Isosteric heats of adsorption (Q_{st}) for a) CO_2 and b) CH_4, in HKUST-1 (black lines) and hB-HKUST-1 (red lines)

At higher pressures (higher gas loading), adsorbate–adsorbate interactions should become non-negligible, thus adsorbent–adsorbate and adsorbate–adsorbate interaction energies can be analyzed. At the highest pressure, CO_2 molecules produced the lowest adsorbent–adsorbate interaction energies of -726.4 and -866.1 kJ.mol^{-1} on the surface of HKUST-1's and hB-HKUST-1, respectively (Figure 5a). Further, its adsorbate–adsorbate interaction energies decreased to -70.6 in HKUST-1 and -75.5 kJ.mol^{-1} in hB-HKUST-1 (Figure 5b). CH_4 produced the lowest adsorbent–adsorbate interaction energies of -184.1 and -168.7 kJ.mol^{-1} on HKUST-1's and hB-HKUST-1's surfaces, respectively (Figure 5c). It also recorded the lowest adsorbate–adsorbate interaction energies of -2.4 in HKUST-1 and -2.2 kJ.mol^{-1} in hB-HKUST-1 (Figure 5d). These values indicate that the adsorption of CO_2 and CH_4 on the MOFs' surfaces were as impressive as their packing inside the pores. This can be seen by the less negative values for the interaction energies of CO_2-CO_2 and CH_4-CH_4 compared to those of these gases on the frameworks. Interaction energies of CO_2-CO_2 demonstrated lower values compared to those of CH_4-CH_4. This implies that CO_2 molecules had stronger adsorbate–adsorbate interactions and were more tightly packed inside the MOFs.

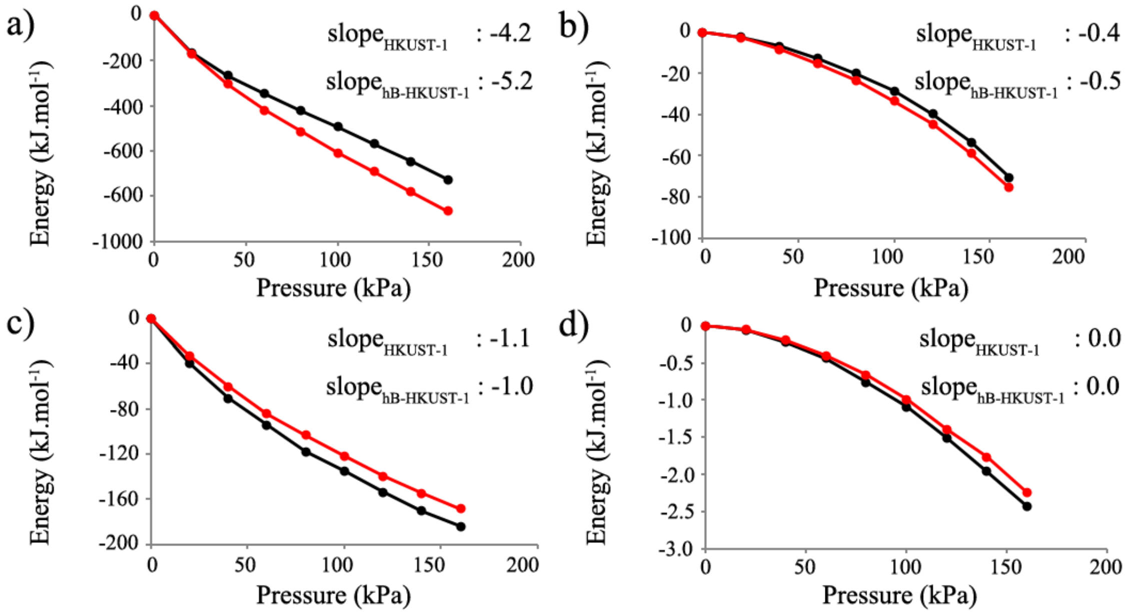

Figure 5. Interaction energies for a) framework - CO_2, b) CO_2 - CO_2, c) framework - CH_4 and d) CH_4 - CH_4. Black and red lines represent HKUST-1 and hB-HKUST-1, respectively.

To explain the adsorbent–adsorbate interactions in more detail, further investigations were carried out. Both the frameworks' surfaces were found to be good platforms for the adsorption of CO_2 as exhibited by the favourable adsorbent–adsorbate interaction energy values. The adsorption of CO_2 on hB-HKUST-1's surface created a considerably lower trend in interaction energy compared to HKUST-1 at pressures over 40 kPa (Figure 5a). In addition, Figure 5c shows that hB-HKUST-1 reduced the adsorption of CH_4. It is suggested that analysis of CH_4 at different pressures be conducted in order to visualize the favourable sites on hB-HKUST-1. Furthermore, HKUST-1 and hB-HKUST-1 showed steeper trend lines for the interaction energy of CO_2 with slopes of -4.2 and -5.2, respectively, compared to those for CH_4 (-1.1 and -1.0, respectively).

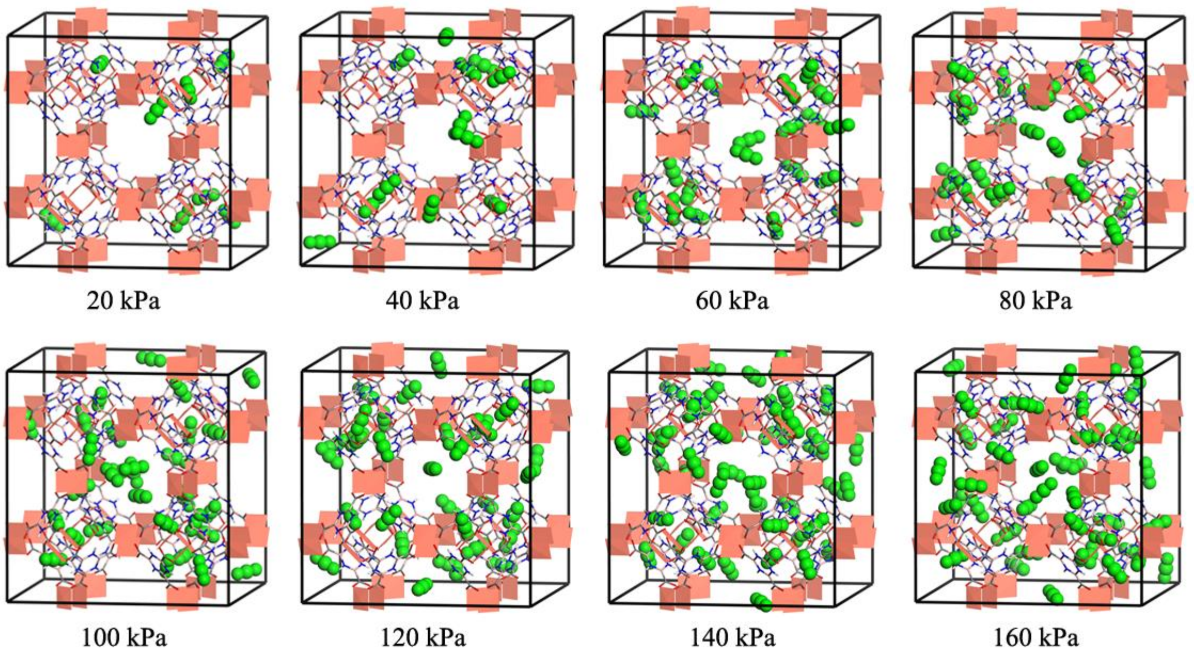
20 kPa
40 kPa
60 kPa
80 kPa
100 kPa
120 kPa
140 kPa
160 kPa

Figure 6. Snapshot diagrams of adsorbed CO_2 gas in hB-HKUST-1 at different pressures. CO_2 molecules are represented by green spheres.

Of the two, hB-HKUST-1 showed slightly better potential for the adsorption of CO_2 gases with increasing pressure. To illustrate the important sites of hB-HKUST-1 for CO_2 adsorption over the range of pressures, examples of snapshots taken from GCMC simulations are depicted in Figure 6. Inspection of these snapshots shows that CO_2 molecules were accommodated within the smaller pores at lower pressures, but did not show any notable aggregation into larger pores. Increasing pressure led to higher loadings of CO_2 in smaller pores where they made more adsorbent–adsorbate interactions on the surface of hB-HKUST-1. Note that some major aggregations of CO_2 were seen in large pores at higher pressures (100, 140 and 160 kPa), caused by adsorbate–adsorbate interactions. On the other hand, CO_2 molecules entered the smaller pores of HKUST-1 at lower pressures (20, 40 and 60 kPa), which resulted in interactions with the framework's surface. With increasing pressure, CO_2 molecules entered the largest pores and created major aggregations at 140 kPa. This supports the higher loading and lower framework-gas interaction energies of CO_2 observed inside hB-HKUST-1, especially at higher pressures.

CONCLUSION

In this study, we found that the use of a hypothetical borazine-based HKUST-1 (named hB-HKUST-1) for CO_2 adsorption was an improvement over the HKUST-1 MOF. However, replacing the benzene ring with borazine in the organic linker did not show a significant difference in its adsorption of CH_4. The average loading of CO_2 gas in hB-HKUST-1 reached 204.9 $mg.g^{-1}$ (4.7 $mol.kg^{-1}$) at 160 kPa, which was relatively higher than the reported experimental value of ~3.7 $mol.kg^{-1}$ at 160 kPa and 303 K [22]. Adsorption of CO_2 in hB-HKUST-1 was mainly governed by adsorbent–adsorbate interactions. We found that smaller pores in hB-HKUST-1 were the most favourable locations for accommodating CO_2 gas. It is clear that borazine-based MOFs have the potential to be a better alternative for adsorption of polar guest molecules. However, this MOF is currently still considered hypothetical, and thus needs to be synthesised to confirm these findings.

REFERENCES

1. Khan, N. A., Hasan, Z. and Jhung, S. H. (2013) Adsorptive removal of hazardous materials using metal-organic frameworks (MOFs): a review. *J. Hazard. Mater.*, **244**, 444–456.

2. Mohamedali, M., Nath, D., Ibrahim, H. and Henni, A. (2016) Review of recent developments in CO2 capture using solid materials: metal organic frameworks (MOFs). *Greenh. Gases*, **115–154**.

3. Abtab, S. M. T., *et al.* (2018) Reticular chemistry in action: A hydrolytically stable MOF capturing twice its weight in adsorbed water. *Chem.*, **4(1)**, 94–105.

4. Li, J., Bhatt, P. M., Li, J., Eddaoudi, M. and Liu, Y. (2020) Recent progress on microfine design of metal–organic frameworks: Structure regulation and gas sorption and separation. *Adv. Mater.*, **32(44)**, 2002563.

5. Jasuja, H., Zang, J., Sholl, D. S. and Walton, K. S. (2012) Rational tuning of water vapor and CO2 adsorption in highly stable Zr-based MOFs. *J. Phys. Chem. C*, **116(44)**, 23526–23532.

6. Karra, J. R. and Walton, K. S. (2010) Molecular simulations and experimental studies of CO2, CO, and N2 adsorption in metal− organic frameworks. *J. Phys. Chem. C.*, **114(37)**, 15735–15740.

7. Orellana-Tavra, C., Köppen, M., Li, A., Stock, N. and Fairen-Jimenez, D. (2020) Biocompatible, Crystalline, and Amorphous Bismuth-Based Metal–Organic Frameworks for Drug Delivery. *ACS Appl. Mater. Interfaces*, **12(5)**, 5633–5641.

8. McDonald, T. M., Lee, W. R., Mason, J. A., Wiers, B. M., Hong, C. S. and Long, J. R. (2012) Capture of carbon dioxide from air and flue gas in the alkylamine-appended metal–organic framework mmen-Mg2 (dobpdc). *J. Am. Chem. Soc.*, **134(16)**, 7056–7065,.

9. Stock, A. and Pohland, E. (1926) Borwasserstoffe, VIII. Zur Kenntnis des B2H6 und des B5H11. *Berichte der Dtsch. Chem. Gesellschaft (A B Ser.)*, **59(9)**, 2210–2215.

10. Chen, P., Lalancette, R. A. and Jäkle, F. (2012) π-Expanded Borazine: An Ambipolar Conjugated B–π–N Macrocycle. *Angew. Chemie Int. Ed.*, **51(32)**, 7994–7998.

11. Fasano, F., *et al.* (2021) BN-Doped Metal–Organic Frameworks: Tailoring 2D and 3D Porous Architectures through Molecular Editing of Borazines. *Chemistry*, **27(12)**, 4124.

12. Lin, K. -S., Adhikari, A. K., Ku, C. -N., Chiang, C. -L. and Kuo, H. (2012) Synthesis and characterization of porous HKUST-1 metal organic frameworks for hydrogen storage. *Int. J. Hydrogen Energy*, **37(18)**, 13865–13871.

13. Lu, W., *et al.* (2014) Tuning the structure and function of metal–organic frameworks via linker design. *Chem. Soc. Rev.*, **43(16)**, 5561–5593,.

14. Hendon, C. H. and Walsh, A. (2015) Chemical principles underpinning the performance of the metal–organic framework HKUST-1. *Chem.*

Sci., **6(7)**, 3674–3683,.

15. Dubbeldam, D., Calero, S., Ellis, D. E. and Snurr, R. Q. (2016) RASPA: molecular simulation software for adsorption and diffusion in flexible nanoporous materials. *Mol. Simul.*, **42(2)**, 81–101.

16. Yakovenko, A. A., Reibenspies, J. H., Bhuvanesh, N. and Zhou, H. -C. (2013) Generation and applications of structure envelopes for porous metal–organic frameworks. *J. Appl. Crystallogr.*, **46(2)**, 346–353.

17. Martin, M. G. and Siepmann, J. I. (1998) Transferable potentials for phase equilibria. 1. United-atom description of n-alkanes. *J. Phys. Chem. B.*, **102(14)**, 2569–2577.

18. Wilmer, C. E. and Snurr, R. Q. (2011) Towards rapid computational screening of metal-organic frameworks for carbon dioxide capture: Calculation of framework charges via charge equilibration. *Chem. Eng. J.*, **171(3)**, 775–781.

19. Saha, D., Bao, Z., Jia, F. and Deng, S. (2010) Adsorption of CO2, CH4, N2O, and N2 on MOF-5, MOF-177, and zeolite 5A. *Environ. Sci. Technol.*, **44(5)**, 1820–1826.

20. Xu, Z., *et al.* (2020) A robust Th-azole framework for highly efficient purification of C 2 H 4 from a C 2 H 4/C 2 H 2/C 2 H 6 mixture. *Nat. Commun.*, **11(1)**, 1–9.

21. Al-Jadir, T. M. and Siperstein, F. R. (2018) The influence of the pore size in Metal− Organic Frameworks in adsorption and separation of hydrogen sulphide: A molecular simulation study. *Microporous Mesoporous Mater.*, **271**, 160–168.

22. Teo, H. W. B., Chakraborty, A. and Kayal, S. (2017) Evaluation of CH4 and CO2 adsorption on HKUST-1 and MIL-101 (Cr) MOFs employing Monte Carlo simulation and comparison with experimental data. *Appl. Therm. Eng.*, **110**, 891–900.